Journal of Kufa for Chemical Sciences Vol. (4) No. (2) ………………….……….Jun. 2025

Article

Synthesis and characterization of a new azo ligand and study of the biological activity, antioxidant and anticancer of the complex Au(III)

Zainab Ghanim Abd[1] Layla Ali Mohammed[2]

1Ph.D-Student ,Part of Thesis, Department of Chemistry, ,College of Education for Girls, University of Kufa , Iraq.

2Advisor, Part of Thesis, Department. of Chemistry, College of Education for Girls, University of Kufa, Iraq

E.mail/ zainabghanimabd@gmail.com

laila.alameri@uokufa.edu.iq

Abstract:

Several metal complexes were synthesized by coordinating the following ions: Co(II), Ni(II), Cu(II), Zn(II), Cd(II), Hg(II), Au(III), and Ag(I), with a newly developed azo ligand obtained from 4-aminosulfonamide and 4-hydroxybenzaldehyde. The ligand structures and their transition metal complexes were characterized using various analytical techniques, including molar conductivity, element microanalysis (CHN), electronic spectroscopy, magnetic sensitivity, nuclear magnetic resonance, infrared spectroscopy, and mass spectrometry. The data indicate that the structures of these complexes is [[M(L)2(H2O)2, where M = Co (II), Ni (II), Cu (II), Cd (II), and Hg (II), [ML(H2O)2] where M = Ag(I), and [M(L)Cl2]] where M = Au(III). The magnetic susceptibility and electronic spectrum data for the complexes suggest an octahedral geometry for all except Au(III), which has a planar square geometry, and Ag(I), which has a planar square geometry. The infrared spectrum results show that the coordination sites are the azo-nitrogen atom and the farther azo-nitrogen atom. The azo ligand is a bidentate structure. The Au(III) complexes exhibit radical scavenging activity for DPPH, indicating potential and promising antioxidant activity. Additionally, the gold complex has shown anti-cancer effects by effectively killing lung cancer cells without affecting healthy cells. This is a significant finding in the potential use of gold complexes as highly selective treatments for lung cancer.

Keywords: novel ligand complexes, azo ligand, antioxidant, anticancer.

1. Introduction

Sulfonamide compounds have attracted the attention of researchers over the past few decades due to their potent biological effects, including antibacterial, anticancer, antithyroid, hypoglycemic, anti-fungal, anti-retroviral, and anti-HIV properties [1]. Similarly, azo dye derivatives have also shown a diverse range of biological activities, such as anti-inflammatory [2], antiviral, antimicrobial [3], antioxidant, and anticancer effects [4]. Azo compounds are a prominent category of chemical compounds that have undergone thorough investigation in scientific research. These substances are quite vibrant and have been employed as pigments for an extended period. Due to their economic and versatile nature, azo compounds have been of great interest in the past few decades, particularly in revealing the preferred coordination geometry of metal complexes, thanks to their structural diversity and accessibility [4- 8]. Therefore, they play a crucial role in determining the selected geometries for chelation of metal complexes. It is recognized that these compounds have been effective in the field of biological complexes of copper (II) for treating rheumatoid arthritis and have also demonstrated anti-ulcer efficiency. This is because they can prevent gastrointestinal irritation, which is a common side effect of other anti-arthritis medications. Azo compounds are also widely used in industries such as textile, dyeing, analytical chemistry, food technology, and pharmaceutical applications [3-10]. They are also used in analytical pH as a calibration to measure complexity, oxidation, or indices. The effectiveness of azo compounds in various biological applications has led to their use in the treatment of textile materials, as well as in the medical field for their antibacterial, antineoplastic, antiseptic, and anti-inflammatory properties [11-14]. They have also been used in the production of medical drugs for diabetes, inflammation, and cancer, such as triple gold complexes, which have shown high inhibitory effectiveness. Additionally, azo compounds have been recognized for their antioxidant properties [15-17]. In this research paper, a sulfonyl amide derivative was prepared, along with several metal complexes, and the triple gold compound was selected for testing its bio-efficacy as an antioxidant and anti-inflammatory agent. The results were promising, and the study was conducted in vitro.

2. Experimental and Materials

The materials used in this study were supplied by Sigma Aldrich and BHD without undergoing a purification process. The melting points and assemblies of the ligand were determined using a thermoelectric model IA-9300 melting point device. The initial analysis was performed using the 1180 C.H.N. 1700 microanalysis unit. Shimadzu's dual-beam UV spectrophotometer captured electronic spectra. The Shimadzu FTIR-8400 spectrophotometer was used to obtain Fourier transform infrared (FTIR) spectra. The spectra were collected in the range of 4000-400 cm $^{-1}$ and KBr disks were utilized. ^{1} H-NMR and ^{13} C-NMR spectra were recorded in ppm units on the Brooker Ultra shield 3000MHz spectrometer, using DMSO-d6 as a solvent. Mass spectra were obtained using the AB Sciex Q-Trap 3200 LC-MS/MS system. Magnetic sensitivity measurements were made using the Faraday method and an MSB-MKI magnetic scale. Pascal constants were utilized to make magnetic adjustments.

2.1. Synthesis of Azo Ligand

Azo ligand was synthesized using the nitration process of 4-aminosulfonamide. Initially, a quantity of 1.72 grams (equivalent to 0.01 moles) of 4-aminosulfonamide was dissolved in a solution containing 3 mL of strong hydrochloric acid and 30 mL of distilled water. Subsequently, the mixture was cooled to a temperature range of 0–5 °C using an ice bath and subjected to continuous stirring. for 15 minutes. Next, a solution of 0.7 g (0.01 mol) of sodium nitrite dissolved in 10 mL of distilled water was added to the mixture with continuous stirring. After the addition was complete, the solution was left to stand for 30 minutes to complete the nitrification process. A drop of wisdom was then added to the solution with continuous stirring, followed by the addition of 1.22 g (0.01 mol) of 4-hydroxybenzaldehyde solution in 10% sodium hydroxide. This caused the solution to turn dark orange. The reaction mixture was allowed to cool overnight. The pH was adjusted to 6 by adding drop-wise diluted hydrochloric acid. This resulted in the formation of orange precipitate, which was allowed to settle before being filtered and washed multiple times with distilled water to remove any salt formed during the chemical reactions. Subsequently, the product underwent a drying process and was subjected to recrystallization using hot ethanol. The resulting compound had a measured melting point within the range of 117-119°C.

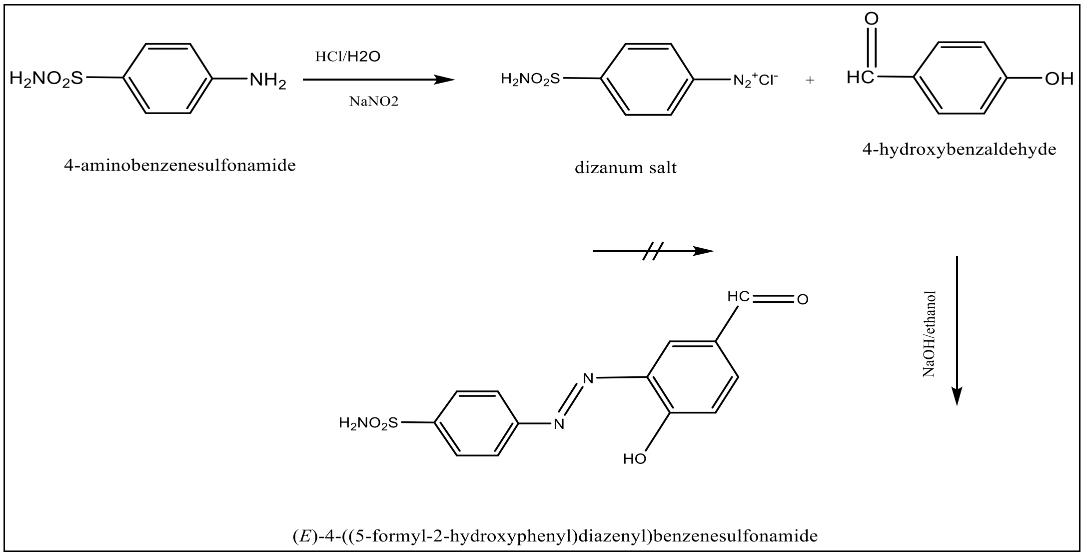

Scheme 1 Ligand azo ligand preparation

2.2 Ligand preparation complexes

(1.172 g) (0.001 mol) of the ligand was dissolved in 30 mL of absolute ethanol and added to (1 mol)(of chlorides of Co(II), Ni(II), Cu(II), Zn(II), Cd (II), Hg (II), Ag (I) and Au(III) dissolved in 25 mL of distilled water in a ratio of (1:2) (ligand: metal), excluding silver and gold. The molar ratio was (1:1). Two drops of an alcoholic solution of ammonium hydroxide were then added to the solution. The mixture was stirred continuously for one hour, allowed to cool, and the collectors were deposited. The mixture was then filtered, air dried, and recrystallized from hot absolute ethanol. Table No. (1) Presents the percentage yield and various physical characteristics of both the ligand and its produced complexes.

Table 1. Physical characteristics of the ligand and complexes

NO	Compounds	Colors	m.p^{0}C	Yalid%
1	HL	Orange	117-119	88
2	[Co (L)$_2$(H2O)2]	yellow	128-130	78
3	[Ni (L)$_2$(H2O)2]	Orange	171-173	70
4	[Cu (L)$_2$(H2O)2]	Orange	125-127	80
6	[Ag((L)(H2O)2Cl]	Orange	130-132	70
7	[Au((L)(H2O)2Cl]	Very Light yellow	123-125	75
8	[Zn (L)$_2$(H2O)2]	Orange-yellow	120-122	80
9	[Cd (L)$_2$(H2O)2]	Dark yellow	158-160	74

2.3.Antioxidant activity

The in vitro free radical scavenging activity of the prepared compounds was evaluated using the (1,1-diphenyl-2-trinitophenylhydrazine) (DPPH) assay [19-21]. First, inventory solutions were prepared and then diluted to different concentrations of methanol (12.5 – 200 mg/ml). Next, a 2 mL methanol solution of the synthetic compound was added to a 0.003% methanol solution (w/v) of DPPH (1 mL). Subsequently, the concoction was briskly agitated and allowed to rest for a duration of 30 minutes. The absorption was measured using ascorbic acid as a standard. The percentage of inhibition (I%) of the test compound was determined using the following formula: I% = (Ac-As)/Ac × 100, where AC is the absorption of the control and As is the absorption of the sample.

3. Methods

The A549 human lung cancer cell line and non-malignant HdFn cells were acquired from the National Cell Bank of Iran, specifically the Pasteur Institute. The cells were grown in RPMI-1640 (GIPCO) and DMEM: medium F12 (GIPCO), with 10% FBS (GIPCO) and antibiotics (100 µg/mL penicillin and 100 µg/mL streptomycin) added. The cells were cultured at a temperature of 37°C in a humid environment containing 5% carbon dioxide. They were subcultured using trypsin/EDTA (Gypco) and phosphate-buffered saline (PBS). Identical media and conditions were employed for both single-layer and three-dimensional cell cultures. The MTT Cell Vitality Test was conducted to assess cell growth and vitality. This test utilized the compound 3-(4,5-dimethylthiazol-2-yl)-2,5-diphenyltetrazolium bromide (MTT) obtained from Sigma-Aldrich Trypsin was employed to enzymatically degrade the cells, which were subsequently gathered and distributed at a concentration of 1.4 x 104 cells/well in 96-well plates, each containing 200 µL of fresh media. The cultures were allowed to incubate for 24 hours. After the cells had formed a single layer, they were exposed to chemicals at concentrations ranging from 400 to 25 µg/mL for 24 hours at a temperature of 37 °C in an environment containing 5% CO2. Following the treatment, the liquid above the sediment was removed and 200 µL of MTT solution (0.5 mg/mL in PBS) was introduced into each individual well. Subsequently, the plate was placed in an incubator set at a temperature of 37°C for an extra duration of 4 hours. The liquid portion was extracted and 100 µL of dimethyl sulfoxide was introduced into each well. The plate was placed on a vibrating device and kept at a temperature of 37°C until the crystals totally dissolved. Cell viability was assessed by quantifying the absorbance at 570 nm using an ELISA reader. The IC50, which represents the concentration of chemicals resulting in 50% cell death, was determined based on the dose-response curves.

4.Results and Discussion

In Table 2, the results of the microelement analysis for the proportional complexes showed a 1:2 [M:L] ratio. The only exceptions were silver and gold, which had a 1:1 ratio. This indicates that the results from the theory were in good agreement with the actual results. To test the purity of the azo compound ligand, elements C, H, and N were analyzed and the TLC technique was used.

4.1.Micro-element analysis

In Table 2, the results of the microelement analysis for the proportional complexes showed a 1:2 [M:L] ratio. The only exceptions were silver and gold, which had a [1:1] ratio. This indicates that the results from the theory were in good agreement with the actual results. To test the purity of the azo compound ligand, elements C, H, and N were analyzed and the TLC technique was used.

Table (2) shows the results of the element almicro-analysis for the ligand and complexes.

NO	Compounds	formala	MWt	Found (Caled) %)			
				C	H	N	M
1	HL	$C_{13}H_{11}$ N_3SO_4	305	51.147	3.606	13.77	
3	[Ni $(L)_2$(H2O)2]	[Ni($C_{26}H_{22}N_3SO_6$)]	702.6	44.440	3.131	5.977	8.340
2	[Co $(L)_2$(H2O)2]	[Co ($C_{26}H_{22}N_3SO_6$]	702.9	44.444	3.121	5.975	8.379
4	[Cu $(L)_2$(H2O)2]	[Cu ($C_{26}H_{22}N_3SO_6$]	707.5	44.223	3.118	5.953	9.0007
5	[Ag((L)(H2O)2Cl]	[Ag($C_{13}H_{12}N_3SO_6$]	447.9	2.902	2.510	8.788	24.090
6	[Au((L)(H2O)2Cl]	[Au(C13H_{11}N3SO6) Cl]	554.5	28.133	1.983	7.574	35.527
7	[Zn $(L)_2$(H2O)2]	[Zn ($C_{26}H_{22}N_3SO_6$]	709	44.005	3.102	5.923	9.167
8	[Cd $(L)_2$(H2O)2]	[Cd ($C_{26}H_{22}N_3SO_6$]	756	41.269	2.910	5.555	7.356
9	[Hg $(L)_2$(H2O)2]	[Hg ($C_{26}H_{22}N_3SO_6$]	844.5	36.944	2.605	4.973	23.718

4.2. Mass spectra

The mass spectra of the synthesis of the Azo ligand and Co (II) were obtained at ambient temperature. The molecular ion peaks obtained confirmed the accuracy of the proposed formula for the composite compounds. The mass spectrum of the ligand revealed a molecular ion peak at 305 m/e (11.11%), corroborating the suggested formula for the compounds. For the molecular formula ($CoC_{26}H_{26}N_6S_2O_{11}$), the mass spectrum of Co (II) also showed a peak of molecular ions at m/z 737.9 (0.1%), which matched the molecular weight of Co (II). The results of the microelement analysis, as shown in Figure 1, further supported this.

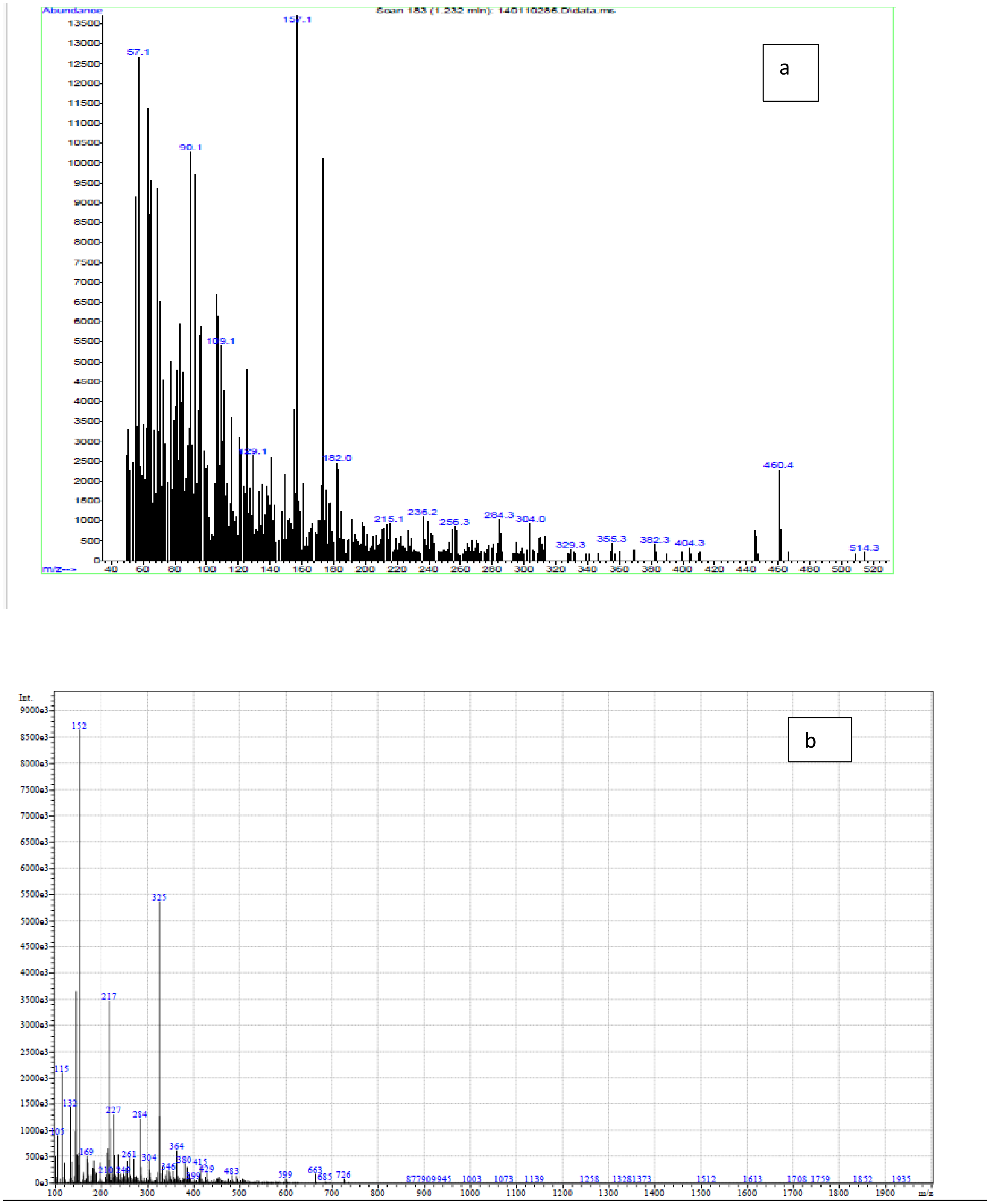

Figure (1) : (a) Mass spectra of the azo-ligand**, and (b)** Mass spectra of the Co(II) complex.

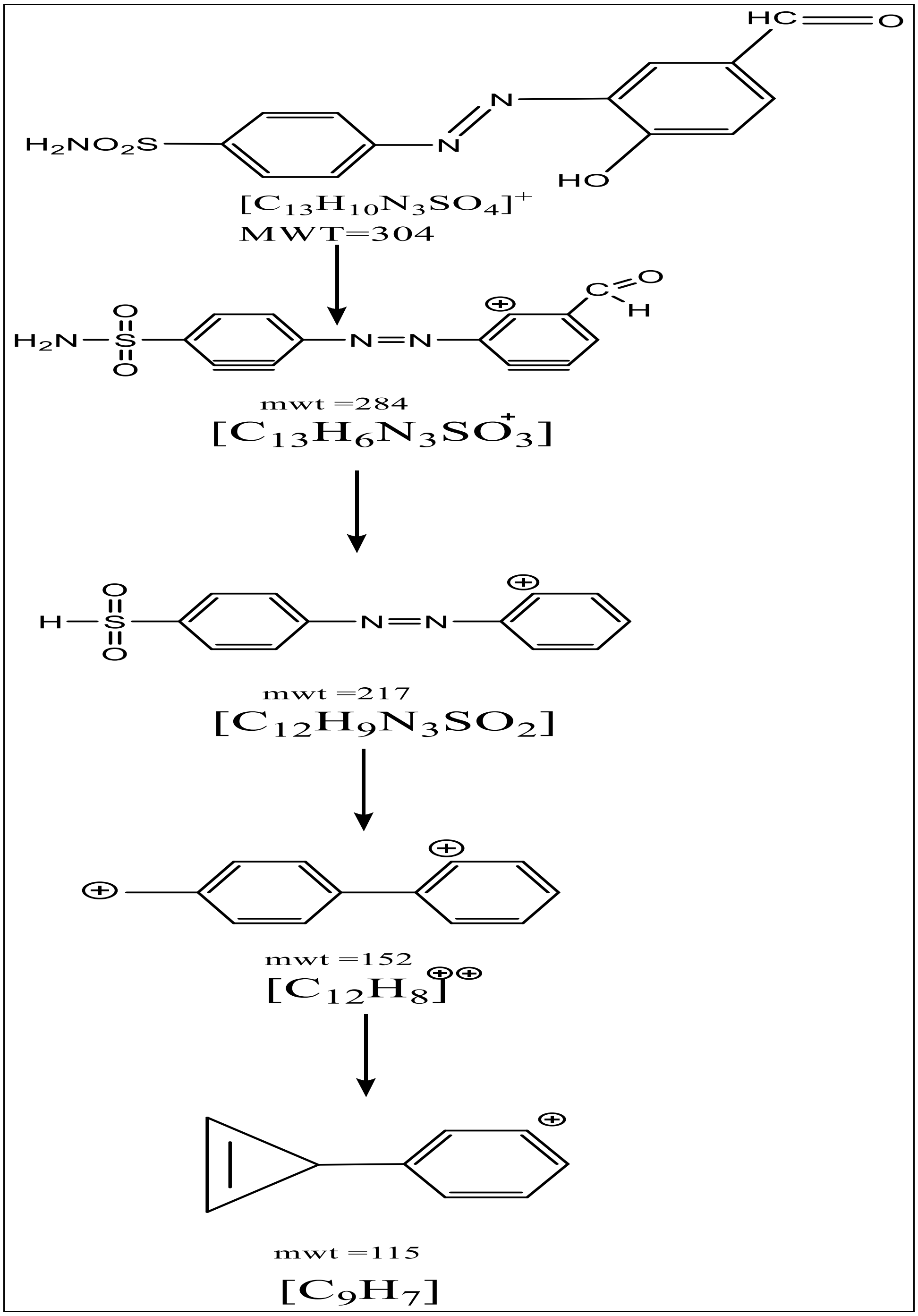

Scheme 2 : Fragment of Azo ligand

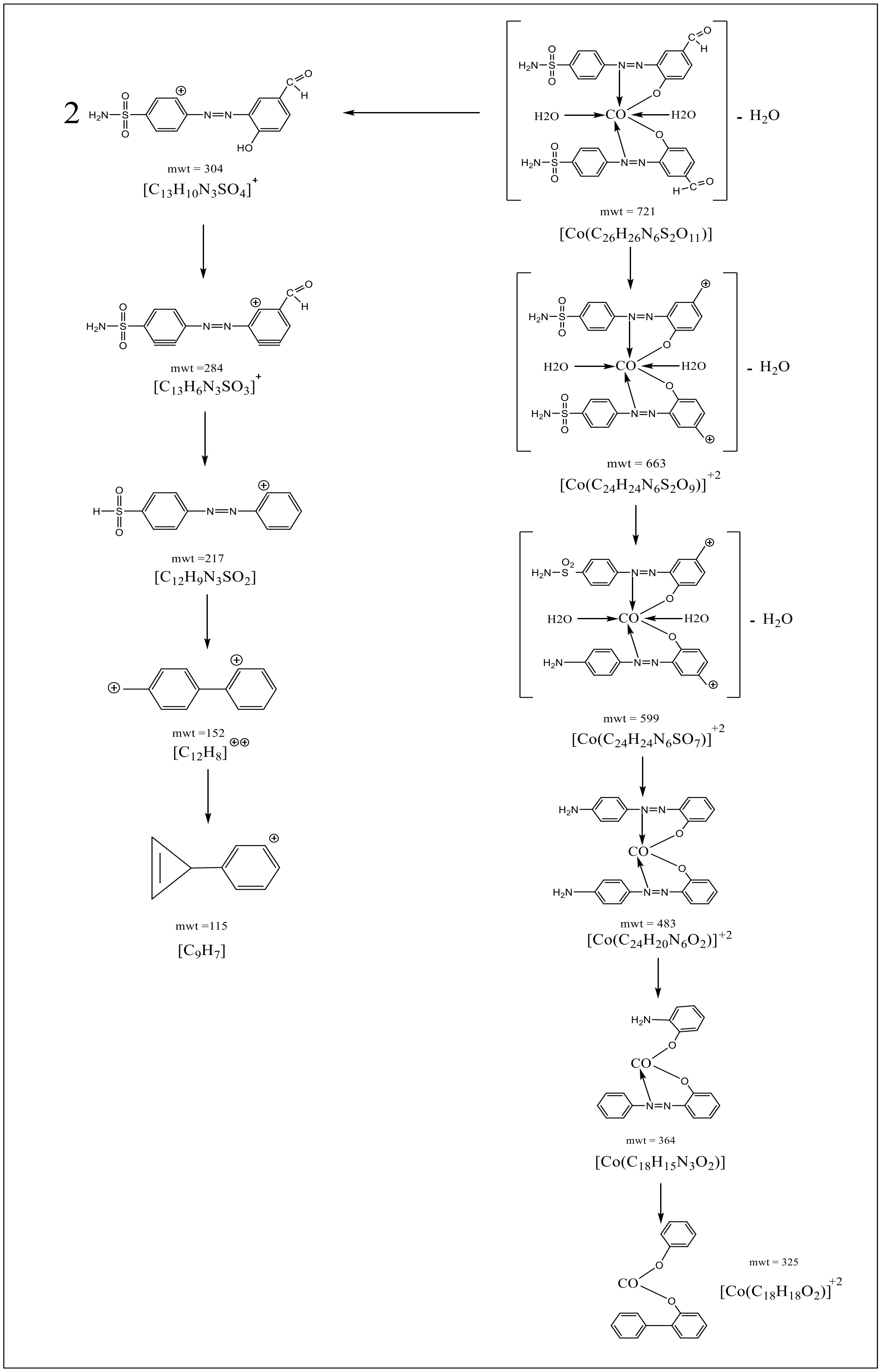

Scheme 3 : Fragment of Co-complex

4.3 ^{1}HNMR Spectra of (a) ligand of (b) Cd complex

The compound's HNMR spectrum was obtained using DMSO-d6 as the solvent. The peak observed at a chemical shift of δ 10.8 ppm can be ascribed to the hydroxide protons. Aromatic protons were observed in the range of δ 7.6 - 8.9 ppm, with multiple signals present. The aldehyde proton at 9.8 ppm and a weak signal at δ 4.9 ppm can be attributed to the proton of the amidalsulfanil group (-NH2) [10,11,12]. The ligand also exhibited a signal at 2.5 ppm, corresponding to the protons of the DMSO-d6 solvent. The zinc complex of the ligand showed similar signals to the ligand itself, with the exception of the hydroxide proton signal, which was absent. This can be explained by the involvement of the hydroxide group in the coordination process. A new signal at 3.3 ppm appeared, which can be attributed to the protons of the water molecule involved in the coordination process, as shown in Figure 2.

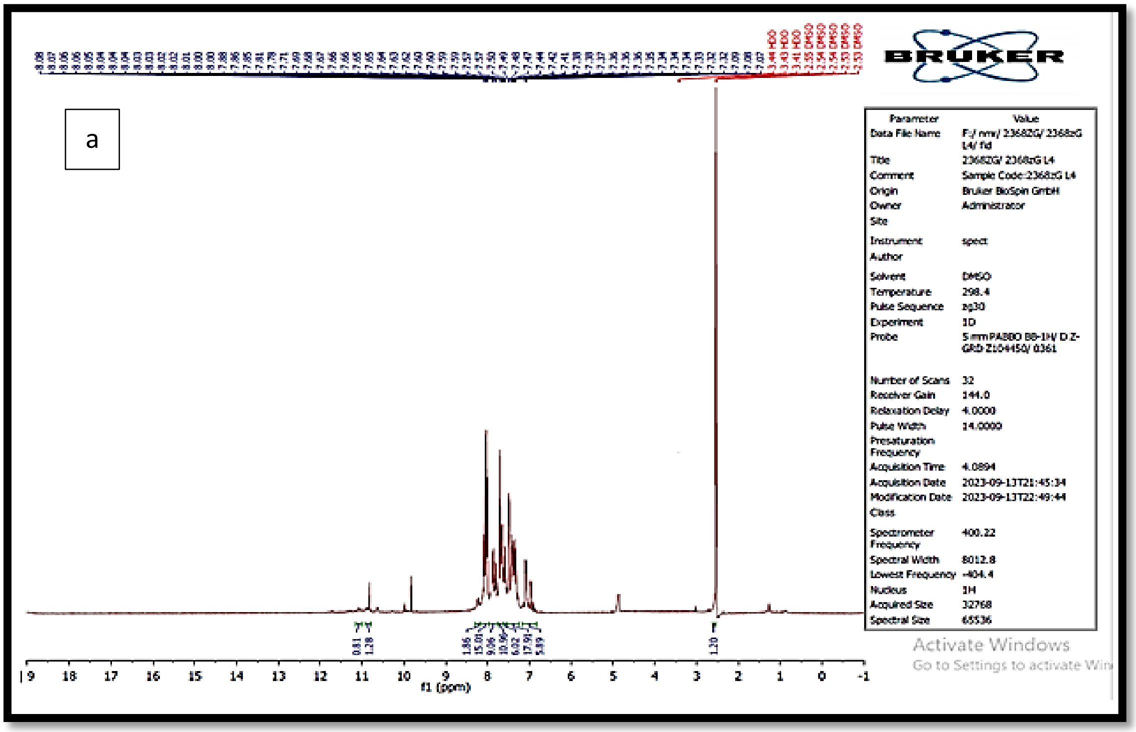

Parameter	Value
Data File Name	F:/ nmr/ 23682G/ 2368zG L4/ fid
Title	23682G/ 2368zG L4
Comment	Sample Code:2368zG L4
Origin	Bruker BioSpin GmbH
Owner	Administrator
Site	
Instrument	spect
Author	
Solvent	DMSO
Temperature	298.4
Pulse Sequence	zg30
Experiment	1D
Probe	5 mm PABBO BB-1H/ D Z-GRD Z104450/ 0361
Number of Scans	32
Receiver Gain	144.0
Relaxation Delay	4.0000
Pulse Width	14.0000
Presaturation Frequency	
Acquisition Time	4.0894
Acquisition Date	2023-09-13T21:45:34
Modification Date	2023-09-13T22:49:44
Class	
Spectrometer Frequency	400.22
Spectral Width	8012.8
Lowest Frequency	-404.4
Nucleus	1H
Acquired Size	32768
Spectral Size	65536

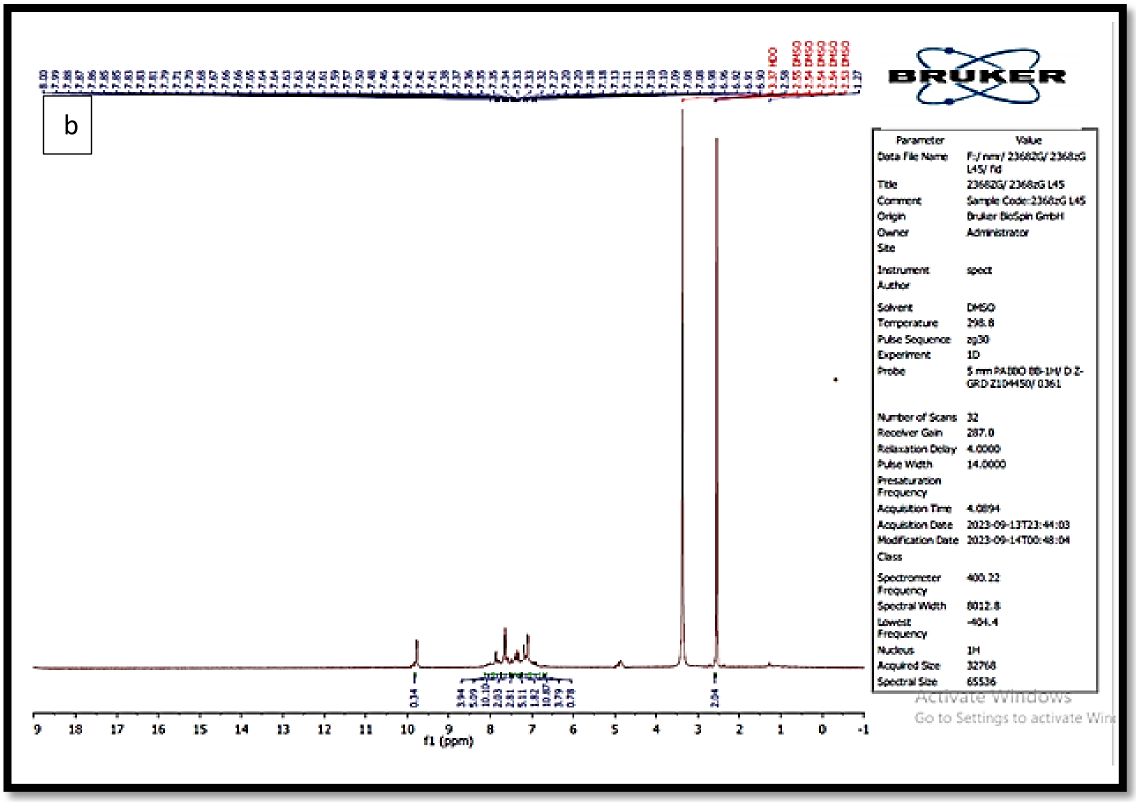

Parameter	Value
Data File Name	F:/ nm/ 23682G/ 2368zG L45/ fid
Title	23682G/ 2368zG L45
Comment	Sample Code:2368zG L45
Origin	Bruker BioSpin GmbH
Owner	Administrator
Site	
Instrument	spect
Author	
Solvent	DMSO
Temperature	298.8
Pulse Sequence	zg30
Experiment	1D
Probe	5 mm PABBO BB-1H/ D Z-GRD Z104450/ 0361
Number of Scans	32
Receiver Gain	287.0
Relaxation Delay	4.0000
Pulse Width	14.0000
Presaturation Frequency	
Acquisition Time	4.0894
Acquisition Date	2023-09-13T23:44:03
Modification Date	2023-09-14T00:48:04
Class	
Spectrometer Frequency	400.22
Spectral Width	8012.8
Lowest Frequency	-404.4
Nucleus	1H
Acquired Size	32768
Spectral Size	65536

Figure (2) The ^{1}HNMR spectrum of (a) ligand and (b) Cd complex

4.4. Infrared spectra

Researchers have used infrared spectroscopy as a highly effective analytical technique to examine the interaction between transition metal ions and organic ligand [13, 14]. By comparing the infrared spectra of metal compounds to those of the free ligand (Table 3), the bonding method between the azo ligand and the specific metal ions can be determined. The free ligand's infrared spectrum (IR) displayed a medium and wide range of approximately (3167, 3057 cm^{-1}), which can be attributed to the presence of (─NH) [15]. This band's position remained consistent in the spectra of the metal chelate compounds, indicating the stability of this group with the metal ions. However, in the Co (II) complex, this band disappeared and was replaced by a new peak at 3353 cm^{-1}, indicating the presence of a coordinated water molecule. Additionally, a new absorption peak at 1625 cm^{-1}, corresponding to ν(H-C═O) of the aldehyde group, was observed. The extended vibration═ at 1444 cm^{-1}, which was present in the free ligand's spectra (22, 23), was also seen in the prepared complexes but with a difference in shape and a decrease in intensity (24). The ligand complexes exhibited distinct new bands in their far infrared spectra, which were absent in the free ligand. These bands were especially observed at (420-445) and (507-580) cm^{-1}, and were ascribed to v(M─N)(23). These findings suggest that the ligand behaves as a binary chelating agent. Figure 3 displays the spectra of the ligand and the compound $[Co(L)_2 Cl_2)]$..

Table 3 lists the ligand and complexes' characteristic IR frequencies in cm^{-1}.

Compound	(OH) H_2O	(NH-)	(-OCH)	(N=N)	)C=C(	)SO_2(	M-N	M-O
$L_{4=}C_{10}H_{16}N_2SO_4$	3350 (OH)	3075 3167	1625	1444	---	1327 1159	-----	----
$[Co(L_4)_2(H_2O)_2]$	3381 931	-----	1625	1406	1589	1336 1163	514	445
$[Ni (L_4)_2(H_2O)_2]$	3381 931	------	1625	1408	1591	1336 1161	514	441
$[Cu (L_4)_2(H_2O)_2]$	3400 910	3352 3209	1625	1408	1591	1334 1161	518	443
$[Zn (L_4)_2(H_2O)_2]$	3479 939	3392 3238	1625	1404	1591	3392 3238	514	420
$[Cd (L_4)_2(H_2O)_2]$	3479 931	3415 3377	1631	1458	1587	1311 1151	507	430
$[Hg (L_4)_2(H_2O)_2]$	3379 939	--	1629	1404	1591	1334 1163	518	420

4.5. Electronic Spectra

The electronic absorption spectra of all substances were measured at room temperature using an ethanol solution in the wavelength range of 200–1100 nm. Table 4 provides a summary of the spectral data for both the Azo ligand and its metal derivatives. The spectral data for the organic bond showed three charge transfer ranges (CT): at 215 nm (46511 cm-1), 256 nm (39062 cm-1), and 345 nm (28985 cm-1). These were caused by the movement of π→π*, →π→π*, and n→π* within the azo ligand. The transition (→π→π*) of the vinyl rings is responsible for the first band's appearance at 215 nm, while the electronic transition (→π→π*) of the group (-N=N-) at 256 nm is responsible for the second band. The third band that appeared in the visible region (345 nm) can be set to transition to n→π*, including the full electronic system of azo dyes. The Co(II) electronic spectrum displays three bands at 894 nm (11,185 cm^{-1}), 641 nm (15,600 cm^{-1}), and 589 nm (16,977 cm^{-1}). These three bands can be assigned to 4T1g(F)→4T2g(F) = v1, 4T1g(F)→4A2g(F) = v2, and 4T1g(F)→4T1g(p) = v3 transitions, respectively. The electron spectrum of the Ni(II) complex displayed three absorption bands: one at a wavelength of 887 nm (corresponding to a wavenumber of 11273 cm-1), another at 751 nm (13315 cm-1), and a third at 422 nm (23696 cm-1). The ranges can be assigned to the transitions 3A2g3T2g(F) (v1), 3A2g3T1g(F) (v2), and 3A2g3T1g(p) (v3), respectively. The spectrum exhibits similarities to the one documented for octahedral complexes. The copper complex (2) exhibited a solitary absorption band in its electronic spectra at a wavelength of 488 nm (20491 cm-1), indicating the occurrence of 2E1g→2T2g transitions. The observations presented suggest that the copper ion (2) exhibits an octahedral distorted shape. The electronic spectra of the Au(III) complex exhibits a solitary band at 410 nm (24,390 cm-1), which can be attributed to 1A1g→1B1g transitions. The electron spectra of the zinc (2), CD (2), and mercury (2) complexes exhibited no transmission as a result of electron saturation (10). Absorptance at 565 nm (17699 cm^{-1}), 522 nm (19157 cm^{-1}), and 665 nm (15037 cm^{-1}) are caused by charge transfer transitions to Zn(II), Cd(II), and Hg(II) complexes, respectively. Figure 4 displays the electronic spectra of the binders and the second copper collector. Figure 4 displays the electronic spectra of the ligands and the Cu (II) complex. In Table 4.

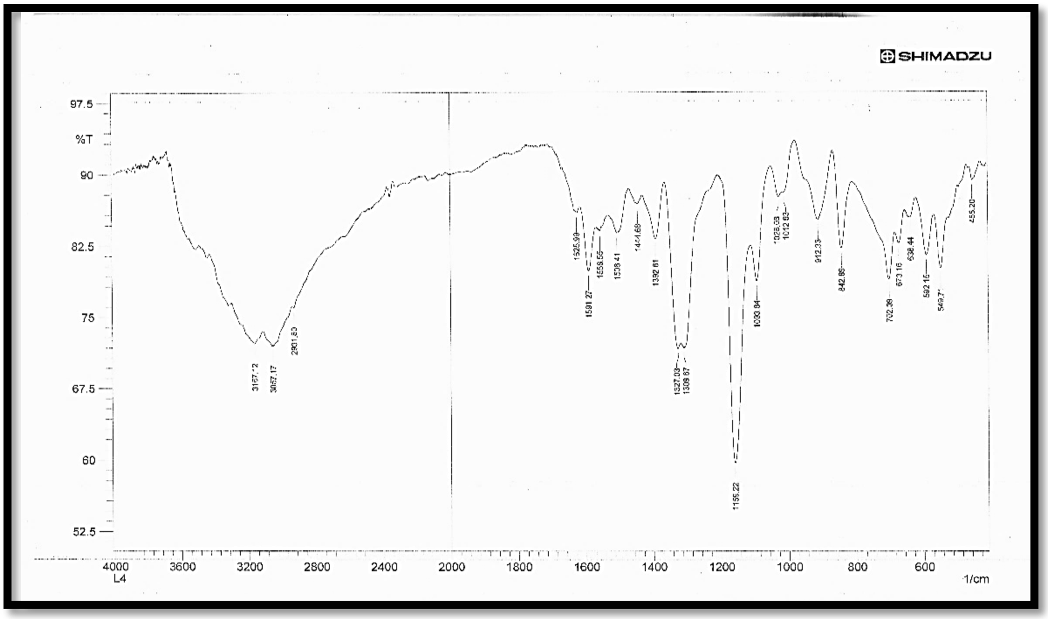
SHIMADZU
97.5
%T
90
82.5
75
67.5
60
52.5
3167.12
3057.17
2981.83
1625.99
1591.27
1556.55
1508.41
1444.68
1392.61
1327.03
1309.67
1155.22
1093.64
1028.03
1012.63
912.33
842.89
702.39
673.16
638.44
592.15
549.71
455.20
4000
L4
3600
3200
2800
2400
2000
1800
1600
1400
1200
1000
800
600
1/cm

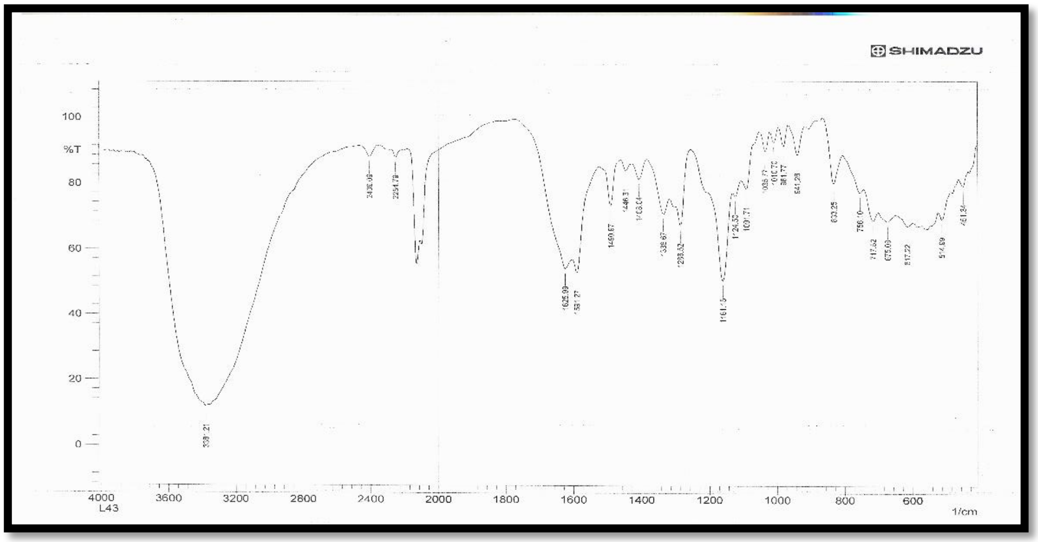
SHIMADZU
100
%T
80
60
40
20
0
3381.21
2408.09
2254.79
1625.99
1591.27
1450.67
1446.31
1403.04
1338.67
1288.52
1161.15
1124.53
1091.71
1035.77
1010.70
981.77
941.28
833.25
756.10
717.52
675.09
617.22
514.89
461.34
4000
L43
3600
3200
2800
2400
2000
1800
1600
1400
1200
1000
800
600
1/cm

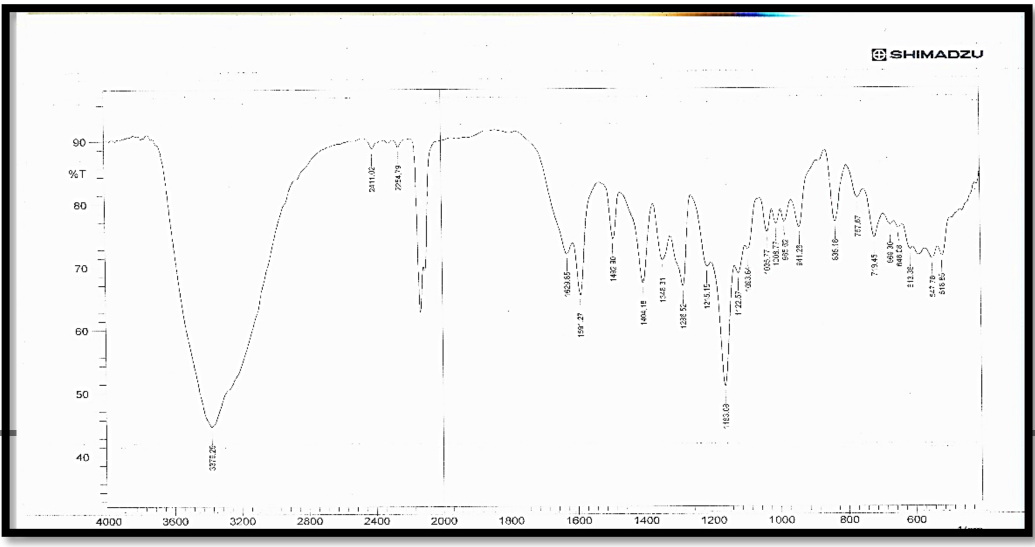
SHIMADZU
90
%T
80
70
60
50
40
3378.26
2411.02
2254.79
1629.85
1591.27
1492.30
1404.18
1346.31
1288.52
1215.15
1163.08
1122.57
1083.64
1035.77
1008.77
985.32
941.28
835.18
767.67
719.45
686.30
648.08
613.36
547.78
516.85
4000
3600
3200
2800
2400
2000
1800
1600
1400
1200
1000
800
600

Figure 4. The spectra of electronic: (a) azo ligand & (b)Ni(II) complex(c) Hg(II) complex

Table.4:Electronic spectra of complexes

Compound	λ (nm)	ύ (cm^{-1})	Transition	Geometry	Hybridization
Ligand	215 256 345	46511 39062 28985	$\pi\rightarrow\pi^*$ $\pi\rightarrow\pi^*$ $n\rightarrow\pi^*$	---------	--------
$(Co(L)_2(H2O)2)$	894 641 589	11185 15600 16977	$^4T_1g(F)\rightarrow {}^4T_2g(F)= v_1$ $^4T_1g(F) \rightarrow {}^4A_2g_{(F)} = v_2$ $^4T_1g(F)\rightarrow {}^4T_1g(p) = v_3$	Octahedral	sp^3d^2
$[Ni(L)_2(H2O)2)$	887 751 422	11273 13315 23696	$^3A_2g \rightarrow {}^3T_2g_{(F)= (\upsilon 1)}$ $^3A_2g \rightarrow {}^3T_1g_{(F)=(\upsilon 2)}$ $^3A_2g\rightarrow {}^3T_1g_{(p)=(\upsilon 3)}$	Octahedral	sp^3d^2
$[Cu (L)_2(H2O)2)]$	488	20491	$^2Eg\rightarrow {}^2T_2g$	Octahedral	sp^3d^2
$[Zn (L)_2(H2O)2)]$	565	17699	M→L,CT	Octahedral	sp^3d^2
$[Cd (L)_2(H2O)2)]$	522	19157	M→L,CT	Octahedral	sp^3d^2
$[Hg(L)_2(H2O)2)]$	665	15037	M→L,CT	Octahedral	sp^3d^2
[Au(L)Cl2]	410	24390	$^1A_1g\rightarrow {}^1B_1g$	Square planer	dSP^2

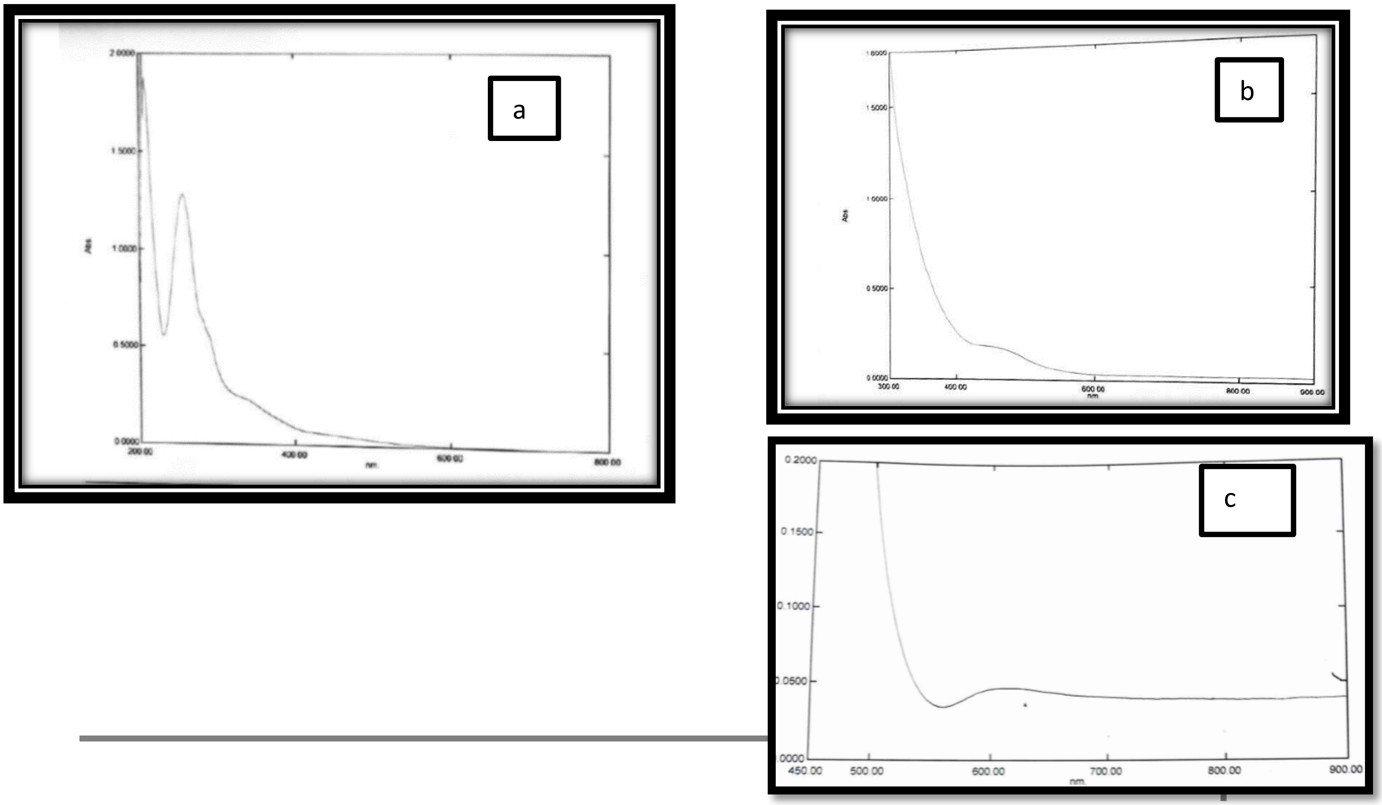

Figure (4) The spectra of electronic : (a) azo ligand & (b)Ni(II) complex (c) Au(III) complex

4.6. Measurement of conductivity

" We performed molar conduction(Λm**)** measurements. On metal complexes in ethanol solvent at a concentration of (10$^{\wedge-3}$ M)and room temperature. The prepared chelate complexes showed a range of conductivity values (4.87-14.6 s.mol$^{\wedge-1}$.cm$^{\wedge 2}$). suggesting that they are non-electrolytic and non-conductive. This information can be used to determine the structures of the complexes

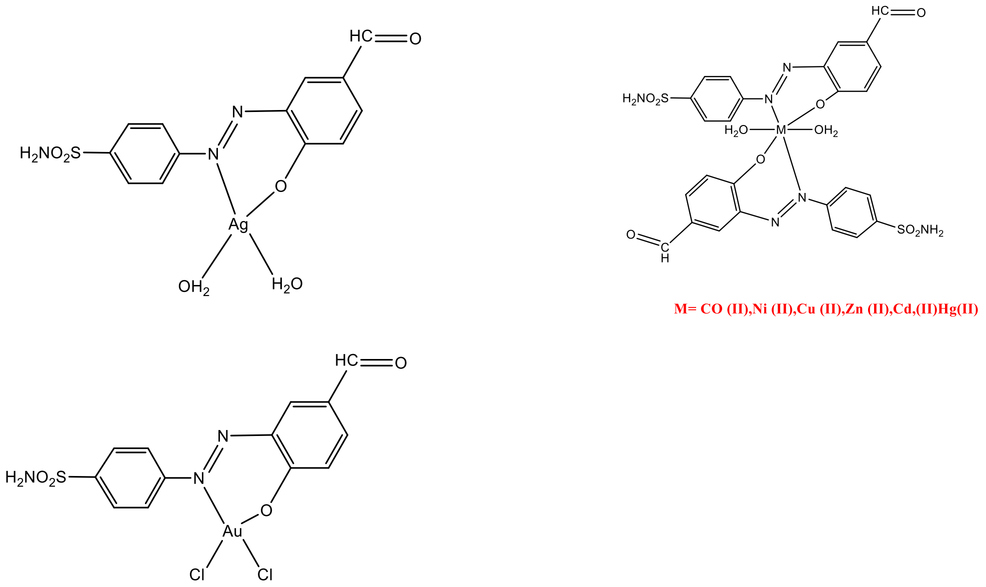

Scheme (4): the proposed structural formula of the complexes

5. Antioxidant activity

Results of scavenging activity for various synthetic compounds are presented in Table 5 and Figure 5. The DPPH test is a commonly used method in laboratories for assessing the effectiveness of antioxidants. DPPH has a peak absorption at 517 nm and disappears when reduced by an antioxidant or becomes a radical. This stable bimagnetic molecule causes a color change from purple to yellow, which serves as an indicator of the hydrogen donation capacity of the tested compounds. Antioxidants can react with DPPH and produce 1,1-biphenyl-2-bicrylhydrazine. The scavenging capabilities of the compounds were determined by their interaction with DPPH at five different concentrations for 30 minutes. Compound Au (III) exhibited the highest scavenging activity, likely due to the presence of the azo group. Alternatives that withdraw electrons typically deactivate aromatic rings and do not have the ability to bind free radicals. The evaluation of antioxidant activity revealed that all the prepared Au (III) complex compounds exhibit antioxidant properties, in comparison to standard antioxidants like ascorbic acid, which was used as a reference in the assessment of their antioxidant activity using the stable free radical method [19,20].

Table.5: Exploration of the scavenging activity of several synthetic compounds

Conc.	Ascorbic acid		L	
(µg/ml)	mean	SD	Mean	SD
200	82.716	2.7783	65.20067	4.050007
100	74.80733	1.446881	52.43067	5.120022
50	64.313	3.142829	44.09733	1.445637
25	52.73933	3.183176	30.55567	4.703107
12.5	39.275	1.351383	17.63133	3.505779

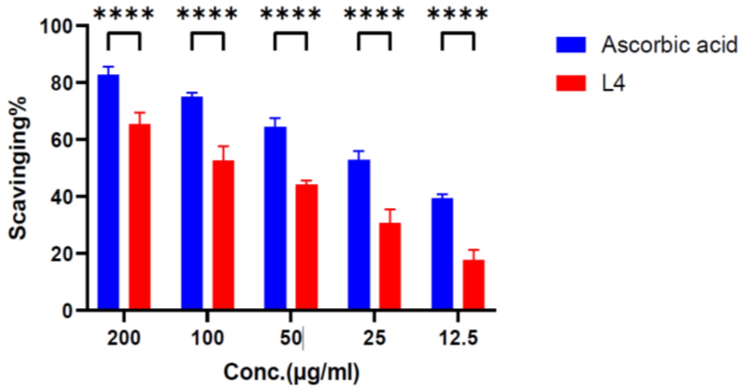

Figure (5) Scavenging activity of the compound using DPPH.

6. Anticancer activity of gold

Various amounts of gold were tested for their cytotoxic efficacy against the lung cancer cell line (A549), in comparison to healthy cells. The anticancer effects of gold were tested at concentrations of 25 mcg, 50 mcg, 100 mcg, 200 mcg, and 400 mcg. As shown in Figure 6 and Table 6, gold's anti-cancer activity increased at higher concentrations. These results are promising when compared to the effects on healthy cells. Previous studies have suggested that the cytotoxic effects of gold are due to its physico-chemical interactions with intracellular proteins, as well as the nitrogen and phosphate groups in DNA [19, 25].

Table (6) The percentage of inhibition(mean) and SD for the Au(III) complex

L	**HdFn**		**A549**	
Conc.(µg/ml)	**mean**	**SD**	**Mean**	**SD**
400	**76.50467**	**4.845775**	**42.978**	**4.462131**
200	**87.92433**	**3.579449**	**51.659**	**2.98794**
100	**92.207**	**2.7783**	**59.6837**	**1.540952**
50	**96.48933**	**1.290811**	**73.9583**	**1.728466**
25	**96.95233**	**1.141793**	**86.7283**	**1.300763**

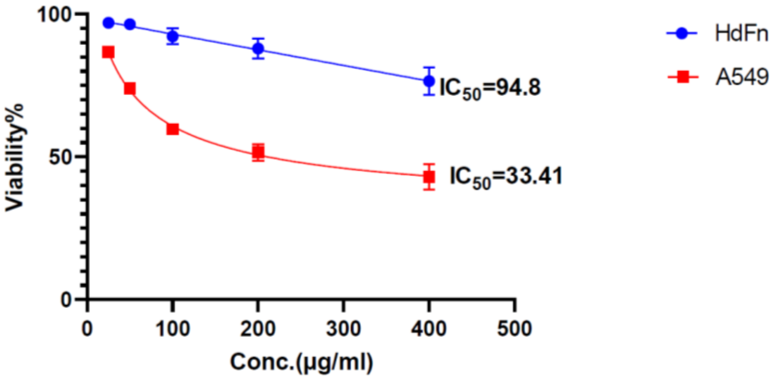

Figure (6): Percentage of inhibition in cells of (a) cancer (A549) line cell against the concentration of complex Au (III)(b) normal line cell(HdFn) against the concentration of complex Au (III)

References

[1] Nagar S, Raizada S, Tripathee N. A review on various green methods for synthesis of Schiff base ligands and their metal complexes. Results Chem. 2023 Dec 1;6.

[2] Muhammad-Ali MA, Jasim EQ, Al-Saadoon AH. Synthesis, Antibacterial Evaluation, and Docking Studies of Some Azo Compounds and Schiff Bases Derived from Sulfonamide. Journal of Medicinal and Chemical Sciences. 2023;6(9):2128–39.

[3] El-Ghamry HA, Al-Ziyadi RO, Alkhatib FM, Takroni KM, Khedr AM. Metal Chelates of Sulfafurazole Azo Dye Derivative: Synthesis, Structure Affirmation, Antimicrobial, Antitumor, DNA Binding, and Molecular Docking Simulation. Bioinorg Chem Appl. 2023;2023.

[4] Van Hoang D, Pham ATT, Nguyen TH, Phan TB, Tran VC. Comparing Thermal Durability and Effects of Annealing Temperature on Characteristics of Hydrogen-Doped ZnO, AZO, and GZO Thin Films. J Nanomater. 2021;2021.

[5] Ashoor LS, Majeed RA, Al-Shemary RKR. "Applications of biological of Azo-Schiff base ligand and its metal complexes and: A review ". Muthanna J Pure Sci. 2021 Jan 13;8(1):74–80.

[6] Wei J, Li Y, Wang M, Yue Q, Sun Z, Wang C, et al. A systematic investigation of the formation of ordered mesoporous silicas using poly(ethylene oxide)-b-poly(methyl methacrylate) as the template. J Mater Chem A Mater. 2013 Aug 21;1(31):8819–27.

[7] Mohsein HF, Majeed NS, Al-Ameerhelal TA. Synthesis and characterization of some new heterocyclic compounds containing a sulfonamide moiety. Res J Pharm Technol. 2019;12(7).

[8] Gómez-Bra A, Gude L, Arias-Pérez MS. Synthesis, structural study and antitumor activity of novel alditol-based imidazophenanthrolines (aldo-IPs). Bioorg Med Chem. 2023 Feb;117563.

[9] Reda MM, Mohammed LA. Preparation, Characterization and studied Biological Effect as Antioxidant of Azo Compound and Schiff base Complexes. Vol. 10, Journal of Survey in Fisheries Sciences.

[10] Kaushik N, Borkar SB, Nandanwar SK, Panda PK, Choi EH, Kaushik NK. Nanocarrier cancer therapeutics with functional stimuli-responsive mechanisms. Vol. 20, Journal of Nanobiotechnology. BioMed Central Ltd; 2022.

[11] Alanazi KD, Alshammari BH, Alanazi TYA, Alshammari OA, Ashmawy AM, Aljohani MM, et al. Green Synthesis of a Novel Cationic Surfactant Based on an Azo Schiff Compound for Use as a Carbon Steel Anticorrosion Agent. ACS Omega. 2023 Dec 26;8(51):49009–16.

[12] Mahmood Aljamali N. Synthesis and Chemical Identification of Macro Compounds of (Thiazol and Imidazol). J Pharm and Tech [Internet]. 2015;8(1). Available from: www.rjptonline.org

[13] Aljamali NM, Abed SM. Bio Studies of Novel Macrocyclic Sulfazan and Linear Sulfazan (Creation, Analysis and Anticancer Assessment). J Pharm Negat Results. 2022;13(4):351–63.

[14] Aljamali DrN, Farhan Z. Anticancer Study of Innovative Macrocyclic Formazan Compounds from Trimethoprim Drug. Egypt J Chem [Internet]. 2022 Apr 20;0(0):0–0. Available from: https://ejchem.journals.ekb.eg/article_232269.html

[15] Aljamali NM, Jawad SF. Preparation, spectral characterization, thermal study, and antifungal assay of (Formazane -mefenamic acid)–derivatives. Egypt J Chem. 2022 Feb 1;65(2):449–57.

[16] Made Wartana I, Agustini NP. Optimal Penetration of RES to the Network by PSO-based Microgrid-Controller How to Cite: I Made Wartana, Ni Putu Agustini (2022). Optimal Penetration of RES to the Network by PSO-based. Vol. 4, International Journal of Applied Engineering & Technology Copyrights @ Roman Science Publications Inc. 2022.

[17] Aad EA, Karaky R, Besombes C, Haddad J, Allaf K. Effect of DIC Technology on Phenolic Content and Antioxidant Activity of Rheum ribes L. rhizome Extracts. Vol. 4, International Journal of Applied Engineering & Technology Copyrights @ Roman Science Publications Inc. 2022.

[18] Hassan QMA, Al-Asadi RH, Sultan HA, Abdullmajed HA, Ali AA, Emshary CA, et al. A novel azo compound derived from ethyl-4-amino benzoate: synthesis, nonlinear optical properties and DFT investigations. 2022; Available from: https://doi.org/10.21203/rs.3.rs-1956241/v1

[19] Plant flavonoids: Classification distribution, biosynthesis, apanelNan S a, TW a, QG a, SL a, LW a, BJ. Classification, distribution, biosynthesis, and antioxidant activity. Plant flavonoids. 2022;383, 132531.

[20] Al Nasr IS, Koko WS, Khan TA, Gürbüz N, Özdemir I, Hamdi N. Evaluation of Ruthenium(II) N-Heterocyclic Carbene Complexes as Enzymatic Inhibitory Agents with Antioxidant, Antimicrobial, Antiparasitical and Antiproliferative Activity. Molecules. 2023 Feb 1;28(3).

[21] Rezk GN, El-Gammal OA, Alrefaee SH, Althagafi I, El-Bindary AA, El-Bindary MA. Synthesis, structural characterization, antioxidant, cytotoxic activities and docking studies of schiff base Cu(II) complexes. Heliyon. 2023 Oct 1;9(10).

[22] Taha Saad S. Synthesis, characterization and theoretical aspects of copper and zinc divalent ion complexes with azo dye derived from 4,5-diphenylimidazole. Bull Chem Soc Ethiop. 2024 Jan 23;38(2):313–23.

[23] Jabbar AI, Al-Jibouri MN, Ismail AH. Synthesis and Structural Studies of Transition Metals Complexes with Poly dentate Azo dye ligand Derived from Coumarine. Egypt J Chem. 2021 Nov 1;64(11):6481–5.

[24] Hasan HA, Alwan WM, Ahmed RM, Yousif EI. Synthesis and Characterization of Some Mixed-Ligand Complexes Containing Azo Dye and 1,10-phenanthroline with Co II , Zn II , Cd II and Hg II Ions. Vol. 28, & Appl. Sci. 2015.

[25] Gavali L V., Mohammed AA, Al-Ogaili MJK, Gaikwad SH, Kulkarni M, Das R, et al. Novel terephthalaldehyde bis(thiosemicarbazone) Schiff base ligand and its transition metal complexes as antibacterial Agents: Synthesis, characterization and biological investigations. Results Chem. 2024 Jan 1;7.